Published in final edited form as:

Biochem J. 2011 August 15; 438(1): 39–51. doi:10.1042/BJ20110129.

TARGETING THE AUTOLYSIS LOOP OF UROKINASE-TYPE PLASMINOGEN ACTIVATOR WITH CONFORMATION-SPECIFIC MONOCLONAL ANTIBODIES

Kenneth A. Botkjaer[*,†], **Sarah Fogh**[*,†], **Erin C. Bekes**[‡], **Zhuo Chen**[*,†], **Grant E. Blouse**[†], **Janni M. Jensen**[†], **Kim K. Mortensen**[†], **Mingdong Huang**[*,§], **Elena Deryugina**[‡], **James P. Quigley**[‡], **Paul J. Declerck**[‖], and **Peter A. Andreasen**[*,†,¶]

[*]Danish-Chinese Centre for Proteases and Cancer; Aarhus University, Aarhus, Denmark

[†]Department of Molecular Biology, Aarhus University, Aarhus, Denmark

[‡]Department of Cell Biology, The Scripps Research Institute, La Jolla, CA, USA

[§]State Key Laboratory of Structural Chemistry, Fujian Institute of Research on the Structure of Matter, Chinese Academy of Sciences, Fuzhou, China

[‖]Laboratory for Pharmaceutical Biology, Faculty of Pharmaceutical Sciences, Katholieke Universiteit Leuven, Leuven, Belgium

SUMMARY

Tight regulation of serine proteases is essential for their physiological functions and unbalanced states of protease activity have been implicated in a variety of human diseases. One key example is the presence of urokinase-type plasminogen activator (uPA) in different human cancer types, with high levels correlating with a poor prognosis. This observation has stimulated efforts into finding new principles for intervening with uPA's activity. We have now characterised the so-called autolysis loop in the catalytic domain of uPA as a potential inhibitory target. This loop was found to harbour the epitopes for three conformation-specific monoclonal antibodies, two with a preference for the zymogen form pro-uPA, and one with a preference for active uPA. All three antibodies were shown to have overlapping epitopes, with three common residues being crucial for all three antibodies, demonstrating a direct link between conformational changes of the autolysis loop and the creation of a catalytically mature active site. All three antibodies are potent inhibitors of uPA activity, the two pro-uPA-specific ones by inhibiting conversion of pro-uPA to active uPA and the active uPA-specific antibody by shielding the access of plasminogen to the active site. Furthermore, by immunofluorescence, the conformation-specific antibodies, mAb-112 and mAb-12E6B10, enabled us to selectively stain pro-uPA or active uPA on the surface of cultured cells. Moreover, in various independent model systems, the antibodies inhibited tumour cell invasion and dissemination, providing evidence for the feasibility of pharmaceutical intervention with serine protease activity by targeting surface-loops that undergo conformational changes during zymogen activation.

[¶]To whom correspondence should be addressed: Department of Molecular Biology, University of Aarhus, Gustav Wied's Vej 10C, 8000 Aarhus C, Denmark. Tel.: +45 8942 5080, Fax: +45 8612 3178. pa@mb.au.dk.

Keywords

antibody; cancer; conformation; immunofluorescence; urokinase-type plasminogen activator; zymogen

INTRODUCTION

Many serine proteases with a trypsin-like fold have important pathophysiological functions. Development of new therapeutics for intervention with these are therefore of great interest. The widely used strategy of developing small molecule inhibitors targeting the catalytic site has proved a daunting task since the catalytic site topology of different proteases are often very similar, making it difficult to obtain sufficient specificity. One strategy to overcome this difficulty is to target other steps in the natural regulation of serine protease activity.

In nature, a key mechanism for the regulation of serine proteases is targeted activation of the initially secreted zymogens or proenzymes. Zymogen activation allows for rapid amplification of the activation signal and generally occurs by cleavage of the bond between amino acid residues 15 and 16 (using the chymotrypsin template numbering). The new amino terminus inserts into a hydrophobic binding cleft forming, in addition to hydrophobic interactions, a salt bridge to the side chain of Asp194 which stabilises the substrate binding pocket and oxyanion hole in a catalytically productive conformation. X-ray crystal structure analyses of trypsinogen and trypsin as well as chymotrypsinogen and chymotrypsin showed that conformational changes after cleavage involve four loop regions collectively called the activation domain, including the activation loop (residues 16–21), the autolysis loop (residues 142–152), the oxyanion stabilizing loop (residues 184–194), and the S1 entrance frame (residues 216–223). The catalytic activity of a zymogen relative to the mature protease is in general the result of an equilibrium between active and inactive conformational states of the protease domain involving these four surface loops (for reviews, see [1] and [2]).

The termination of serine protease activity is likewise a key physiological regulatory event, with inhibition mainly occurring by other proteins with loops that can bind covalently or non-covalently to the active site of the proteases. Inhibitors of the serpin family are an important example of such regulatory proteins. Of crucial importance for the inhibitory mechanism of serpins is the surface-exposed reactive centre loop (RCL), tethered between β-strands 1C and 5A. The active site of the protease binds to the P1-P1’-bond of the RCL to form a non-covalent Michaelis complex, attacks it as a substrate, but at the enzyme-acyl intermediate stage, the N-terminal part of the RCL inserts as β-strand 4, thereby pulling the protease to the opposite pole of the serpin and distorting its active site so that it is unable to complete the catalytic cycle (for reviews, see [3];[4];[5]).

A serine protease of particular relevance is urokinase-type plasminogen activator (uPA), which catalyses the conversion of plasminogen to the active protease plasmin that in turn directly catalyses the degradation of extracellular matrix proteins. Abnormal expression of uPA is implicated in tissue remodelling in several pathological conditions, and in particular, uPA is central to the invasive capacity of malignant tumours (for reviews, see [6];[7];[8]).

As with all trypsin-like proteases, uPA has a catalytic serine protease domain, with surface-exposed loops around residues 37, 60, 97, 110, 170, and 185. Besides the catalytic domain, uPA has an amino-terminal extension consisting of a kringle domain and an epidermal growth factor domain. The latter domain functions in binding to the cell surface-anchored uPA receptor (uPAR) (for a review, see [8]). Several proteases including plasmin (for a review, see [8]), glandular kallikrein [9], matriptase [10], and hepsin [11] can catalyse the activation of the zymogen, pro-uPA. The primary inhibitor of uPA is the serpin plasminogen activator inhibitor-1 (PAI-1). Whereas several three-dimensional structures of the catalytic domain of uPA in the active conformation have been determined by X-ray crystal structure analysis, the structure of pro-uPA remains to be reported and details of zymogen activation are therefore still unclear.

Conformational changes in proteases induced by events such as zymogen activation and cofactor binding have previously been studied using conformation-sensitive antibodies as probes. In a study of factor VIIa, it was found that binding of a monoclonal antibody was affected by conformational transitions of the protease domain [12] and conformational changes of a specific surface residue bound by the antibody was found to be linked to changes in the active site [13]. Furthermore, conformational antibodies have been shown to possess interesting inhibitory mechanisms alternative to standard competitive inhibitors binding at the active site. Using X-ray crystallography, it was found that the antibody Fab40 against the trypsin-like serine protease hepatocyte growth factor activator (HGFA) allosterically inhibits the protease activity by binding to a surface loop keeping the catalytic site in a conformation incompatible with substrate binding [14].

We previously described a conformational monoclonal antibody with a novel mechanism of interfering with the activity of uPA, *i.e.*, by inhibiting conversion of pro-uPA to active uPA [15]. On the basis of this finding and with the dual purpose of elucidating mechanisms of zymogen activation and finding new principles for therapeutic intervention with serine protease activity, we have now performed a functional characterisation of three inhibitory monoclonal antibodies with strongly differential affinity to pro-uPA or active uPA. Mapping of the epitopes was used as means of localising regions changing conformation upon pro-uPA activation as well as by deciphering interaction areas on uPA when reacting with its macromolecular substrate, plasminogen, and inhibitor, PAI-1. The autolysis loop of uPA was found to be important for binding of all three conformation-specific antibodies. Consequently, this loop seems to be strongly implicated in conformational changes during the activation of pro-uPA as well as in uPA´s interaction with plasminogen and PAI-1. Furthermore, the efficacy of regulating uPA protease activity by the different mechanisms employed by the monoclonal antibodies was evaluated in cancer model systems *in vitro* and *in vivo*. Targeting surface-loops outside the conserved catalytic site was found to be a feasible approach for the inhibition of cancer cell invasion and dissemination. Additionally, the differential affinity of the antibodies to pro-uPA or uPA allowed us to detect pro-uPA versus uPA on the surface of human tumour cells by immunofluorescence. Therefore, these antibodies potentially represent new tools for separate analysis of pro-uPA and active uPA levels as relevant biomarkers.

MATERIALS AND METHODS

Buffer conditions

Unless otherwise indicated, all *in vitro* reactions were carried out in a buffer containing 30 mM HEPES, pH 7.4, 135 mM NaCl, 1 mM EDTA and 0.1 % bovine serum albumin (HBS-B) or 0.1 % polyethylene glycol 8000 (HBS-P).

uPA

Human two-chain uPA was purchased from Wakamoto (Tokyo, Japan). Recombinant human pro-uPA was a gift from Abbott Laboratories (IL, USA). The uPA-PAI-1 complex was prepared as described [16]. The pro-uPA-PAI-1 complex was prepared by incubating pro-uPA and PAI-1 (1:2 molar ratio) in the presence of 2 μg/ml aprotinin and 10 mM Ile-Val for 1 hour at 37°C [17]. The complexes were analyzed by SDS-PAGE under reducing conditions, confirming that the uPA in the complex was either in the single-chain pro-uPA-form or in the two-chain active uPA form, as intended.

Recombinant wild type (wt) and mutant recombinant human pro-uPA and active uPA variants were expressed in HEK 293T cells [18]. When expressed under standard conditions, at least 50% of the uPA in the conditioned medium was active uPA, as evaluated by immunoblotting analysis under reducing conditions. When cultured in the presence of 5 μg/ml aprotinin, no conversion of pro-uPA to active uPA was observed. When active uPA was needed, HEK 293T cells were grown in the absence of aprotinin and the pro-uPA in the conditioned medium was after conditioning converted to uPA by adding plasmin. The concentration of uPA variants in the conditioned medium was determined using surface plasmon resonance analysis (see below).

Other proteases

The serine protease domain of recombinant human matriptase (residues 596–855) was purchased from R&D systems (Wiesbaden-Nordenstadt, Germany). Glu-plasminogen purified from human plasma was a kind gift from Lars Sottrup-Jensen (Aarhus University, Denmark).

PAI-1

Human PAI-1 was expressed with an N-terminal His6-tag and purified from *Escherichia coli* cells [19, 20].

Antibodies

Monoclonal antibodies against pro-uPA were generated by i.p. immunisations of Balb/c mice with recombinant human single-chain pro-uPA yielding 22 clones including mAb-101 and mAb-112 [15], or with recombinant human two-chain uPA yielding mAb-12E6B10 [21]. Antibodies were purified from hybridoma conditioned medium using Protein G Sepharose 4FF [22]. One litre of cell culture supernatant yielded between 15 and 50 mg purified antibody.

mAb-PUK was purchased from Technoclone (GmbH, Vienna, Austria).

The following antibodies were also used in this study: mouse anti-uPA mAb-6 [18]; rabbit polyclonal anti-uPA antibody F1609 [23]; mouse anti-PAI-1 mAb-2 [24]; mouse anti-PAI-1 mAb-7 [25] and mouse anti-CD44 mAb 29-7 [26].

Surface plasmon resonance analysis

Surface plasmon resonance (SPR) analyses were performed on a BIACORE T100 instrument, using CM5 sensor chips, flow rates of 30 μL/min, and HBS-B with 0.05 % Tween 20. Concentrations of uPA variants in conditioned media from HEK 293T cells were determined by measuring the initial rate of binding to a chip with 200 response units (RU) of anti-uPA mAb-6 with an epitope in the kringle domain [18], using a standard curve of purified pro-uPA or uPA. Affinities of the antibodies for wt or various forms of mutant pro-uPA and uPA were determined by injecting the proteases (0.5 – 150 nM), either purified or in conditioned media, over a chip with 200 RU of immobilized mAb-112, mAb-101, mAb-PUK or mAb-12E6B10. The k_{on}, ko_{ff} and K_D values were determined by global fitting to a 1:1 binding model with the BIACORE evaluation program.

Binding of the antibodies to a complex between uPA and PAI-1 or between pro-uPA and PAI-1 was assessed by capturing 500 RU of preformed complexes on a chip with anti-PAI-1 mAb-7 immobilized to a final response level of 2000 RU. Binding was then evaluated by injecting the antibodies in concentrations of up to 200 nM.

Binding of the antibodies to pro-uPA or uPA prebound to uPAR was analysed by capturing 300 RU of pro-uPA or uPA on a chip with human soluble uPAR immobilised to a final response of 1700 RU. Binding was evaluated by injecting the antibodies in concentrations of up to 1 μM.

The ability of the various antibodies to compete with each other for the binding to either uPA or pro-uPA was evaluated by immobilising a chip with 200 RU of one antibody and injecting uPA or pro-uPA alone or pre-incubated with an excess of the other antibodies.

In vitro plasminogen activation assay

Pro-uPA or uPA (0.25 nM) was pre-incubated with various concentrations of the antibodies (5–160 nM) at room temperature for 30 minutes in HBS-B. Addition of 0.5 μM Glu-plasminogen and 0.5 mM of the plasmin substrate H-D-Val-Leu-Lys-*p*-nitroanilide (S-2251) initiated the reaction at 37°C. S-2251 hydrolysis was monitored as the increase in absorbance at 405 nm.

Pro-uPA activation assay

Ten nM pro-uPA was incubated in the presence or absence of 100 nM of antibodies at room temperature for 30 minutes in HBS-B. At time zero, 0.5 nM plasmin or 5 nM matriptase was added. Then, the mixtures were incubated at room temperature for the indicated time periods, after which the activity of plasmin and matriptase was quenched by addition of 1 μM aprotinin. The uPA substrate H-D-Glu-Gly-Arg-*p*-nitroanilide (S-2444) was added to a final concentration of 0.5 mM and the amount of active uPA generated during the incubation

with plasmin and matriptase was estimated by the rate of S-2444 hydrolysis and comparison to a standard curve of active two-chain uPA.

Analysis of pro-uPA cleavage by SDS-PAGE and immunoblotting analysis

Samples of pro-uPA (200 nM) were incubated in the presence or absence of 300 nM antibody for 30 min at room temperature in HBS-P. At various times after the addition of 5 nM plasmin, samples were removed and analyzed by reducing SDS-PAGE and immunoblotting with rabbit polyclonal anti-uPA antibody F1609.

Complex formation between pro-uPA and PAI-1 followed by SDS-PAGE

The effect of antibodies on the complex formation between single-chain uPA and PAI-1 was analyzed by pre-incubating pro-uPA with or without a 2-fold molar excess of mAb-PUK, mAb-112 or mAb-101 for 30 minutes at room temperature in HBS-P with 1 μg/mL aprotinin added. The reaction was started by addition of PAI-1 in a 1.5-fold molar excess compared to pro-uPA. After incubation for varying time points, the reaction was stopped by addition of phenylmethylsulfonyl fluoride (PMSF) to a final concentration of 1 mM and boiling for 10 min. The reaction products were analyzed by SDS-PAGE under non-reducing conditions. The resulting protein bands were visualized with Coomassie Brilliant Blue staining. Relative amounts of pro-uPA alone and in complex were quantified by densitometric scanning using Quantity One software (BIO-RAD Laboratories, CA, USA). Reaction rates were evaluated as k_{obs}, the pseudo-first-order rate constant describing the monoexponential approach to complete inhibition, by fitting the data points to equation 1, where $[AB]_t$ is the amount of complex formed between pro-uPA and PAI-1 at time t, $[AB]_{max}$ is the maximal amount of complex that can be formed and t is the reaction time.

$$\frac{[AB]_t}{[AB]_{\max}} = 1 - e^{kobs*t} \quad \text{(Equation 1)}$$

Cell surface-associated plasminogen activation

uPA-catalysed plasminogen activation was assayed with pro-uPA or active uPA bound to uPAR at the surface of U937 cells. U937 cells were cultured as described previously [27], washed, and resuspended for 3 minutes in 50 mM glycine-HCl, pH 3 containing 0.1 M NaCl to remove endogenous pro-uPA and uPA from the cell surface. After washing, the cells were resuspended in HBS-B and distributed into the wells of non-transparent 96-well micro titre plates (Nunc, Roskilde, Denmark) yielding a final cell density of 5×10^6 cells/mL. Cells were preincubated for 15 minutes at 37°C with 200 nM plasminogen and 400 nM α_2-antiplasmin, to restrict plasmin activity to the cell surface, prior to initiating the reactions by adding 1 nM pro-uPA or uPA pre-incubated alone or with mAb-101, mAb-112, mAb-PUK or mAb-12E6B10 at varying concentrations and the fluorogenic plasmin substrate H-D-Val-Leu-Lys-7-amido-4-methylcoumarine (VLK-AMC, 200 μM). The increase in fluorescence was monitored in a Spectromax Gemini fluorescence plate reader (Molecular Devices), using an excitation wavelength of 390 nm and an emission wavelength of 480 nm.

In vitro invasion assays

For the cancer cell invasion assays, PC-hi/diss cells were used [26]. In Matrigel invasion assays, the upper side of a 6.5 mm insert with 8 μm pore Transwell membranes (Fisher Scientific) was pre-coated with 2 μg Matrigel (BD Biosciences). As attractant for cell migration and invasion, conditioned medium from chicken embryonic fibroblasts (CM-CEF) where used. CM-CEF was prepared by growing chicken embryonic fibroblasts in serum-containing medium to confluence with approximately 5×10^4 cells/cm^2. The cells were washed and overlaid with 6 ml of serum-free medium for up to 48 hr before CM-CEF was harvested. CM-CEF was diluted 1:1 with serum-free DMEM (SF-DMEM) and placed in the lower chamber. 1×10^5 PC-hi/diss cells were plated in 100 μl of SF-DMEM on top of the Matrigel in the upper chamber and invasion was allowed for 48 hours at 37°C. After incubation, adherent cells from the underside of the membrane were detached with trypsin/EDTA, combined with non-adherent cells from the lower chamber and counted. Monoclonal antibodies were added to both the upper and lower chambers at 333 nM final concentrations. Aprotinin was used as a positive control for the inhibition of invasion at a concentration of 0.1 trypsin inhibitory units/ml (TIU/ml).

For the three-dimensional tumour escape assay, a drop containing 2.1 mg/ml collagen (type I from rat tail, BD Biosciences) and 25×10^3 PC/Hi-diss cells in SF-DMEM was prepared. After gelation, this drop was then immersed into a mixture containing 3 mg/ml fibrin (fibrinogen from bovine plasma, Sigma-Aldrich, activated by thrombin), 1.5 mg/ml collagen and 20 ng/ml human EGF. Once the droplet-containing matrix had polymerised, AIM-V medium containing 0.01% chicken serum and mAbs (final concentrations of 167 nM) or aprotinin (final concentration of 0.1 TIU/ml) was overlaid. Cells were allowed to escape into the surrounding fibrin/collagen matrix for 10 days at 37°C. The AIM-V medium containing inhibitors was exchanged on day 3 and 7. Images were captured on day 10 with an Olympus microscope equipped with an infinity1 at 10 × original magnification. The number of escaped cells and distance invaded from the original spheroid were quantified by ImageJ [28].

Chicken embryo intravasation assay

The effect of anti-uPA mAbs on the intravasation of human cancer cells in the chicken embryo was analysed as described [26]. Briefly, SPAFAS White Leghorn embryos (Charles River, North Franklin, CT) were allowed to develop for 10 days after which the chorioallantoic membrane (CAM) was dropped and 2.5×10^6 PC-hi/diss cells in 25 μl were applied to the CAM. On day 2 and 4 after tumour cell grafting, 25 μg of mAbs in 100 μl PBS, pH 7.4 (Dulbecco's phosphate buffered saline, Lonza, Walkersville, USA) with 5% dimethyl sulfoxide (DMSO) were added topically to the primary tumours formed on the CAM. On day 7, primary tumours were excised and weighed and the lower CAM harvested for analysis of human cancer cell intravasation quantified by qPCR on primate specific Alu-sequences, as described [26].

Immunocytochemical detection of uPA versus pro-uPA on the surface of PC-hi/diss cells

To discriminate between human pro-uPA and active uPA on the surface of PC-hi/diss cells, the conformation-sensitive antibodies mAb-112 and mAb-12E6B10 were employed in

immunofluorescence microscopy. To this end, 3×10^5 PC-hi/diss cells were seeded on cover slips pre-coated with collagen. The cells were allowed to grow in AIM-V medium alone or in the presence of 0.1 % chicken serum with or without 0.1 U/ml aprotinin. After 2 days of growth, the cells were washed in PBS, fixed with 2 % paraformaldehyde and incubated with PBS containing 2 % BSA and 2 % goat serum to block any unspecific binding. 4 μg/ml of mAb-112, mAb-12E6B10, mouse IgG or anti-CD44 mAb 29-7 (conditioned hybridoma medium from clone 29-7 diluted 1:1) was added to the cells and allowed to bind overnight at 4°C. After washing with PBS, fluorescein isothiocyanate (FITC)-conjugated goat anti-mouse antibody was added and allowed to bind for 1 hour, room temperature. The cell nucleus was stained with 1 μg/ml 4',6-diamidino-2-phenylindole dihydrochloride (DAPI). Pictures were acquired with an immunofluorescence microscope using the same exposure time for all samples. In parallel, samples of conditioned medium from the cells grown under the various conditions were taken and analyzed for the relative amounts of pro-uPA and uPA by reducing SDS-PAGE followed by Western blotting.

RESULTS

Choice of conformation-specific monoclonal antibodies

Three monoclonal antibodies, showing preferential binding affinity towards either pro-uPA or active uPA, were selected for functional characterisation. Two of the antibodies have previously been described: mAb-112 was isolated after immunisation of mice with human pro-uPA [15], and mAb-12E6B10 was isolated after immunisation of mice with human active uPA [21]. A commercially available monoclonal antibody, mAb-PUK, was also characterised. A fourth antibody, mAb-101, binding to the catalytic domain but without preference for neither pro-uPA nor active uPA, was selected to serve as a control. The binding kinetics of the selected antibodies towards pro-uPA and active uPA was determined by surface plasmon resonance (SPR) analysis. As previously reported [15], mAb-112 has a clear preference towards pro-uPA with a K_D that is more than 300-fold lower than that for active uPA (Table 1). mAb-PUK demonstrated highly selective binding towards pro-uPA. In agreement with a previous report [21], mAb-12E6B10 showed selective binding towards two-chain active uPA. The control antibody mAb-101 bound equally well to both forms of uPA (Table 1). mAb-112 competed with mAb-PUK for binding to pro-uPA and with mAb-12E6B10 for binding to active uPA, in the SPR analysis, but none of these three antibodies competed with mAb-101 (data not shown).

Effects of the monoclonal antibodies on plasminogen activation

The functional effects of the antibodies on uPA were investigated in a coupled plasminogen activation assay, in which plasminogen is incubated with pro-uPA or active uPA and plasmin generation scored currently by a chromogenic plasmin substrate. We chose this assay, although it does not allow a strict quantitative analysis, due to the complicated nature of the events taking place. When using pro-uPA, the reaction is initiated by trace amounts of plasmin activating pro-uPA and/or trace amounts of active uPA activating plasminogen. The plasmin formed will activate more pro-uPA and the active uPA formed will generate more plasmin. Moreover, plasmin may convert Glu-plasminogen to Lys-plasminogen, which is a better substrate for active uPA than Glu-plasminogen [29];[30];[31]. In spite of the

qualitative nature of the assay as employed here, it did allow us to distinguish between antibodies inhibiting pro-uPA activation and antibodies inhibiting active two-chain uPA directly. The latter type of antibodies will inhibit the assay initiated with pro-uPA as well as with active uPA, whereas antibodies binding only to pro-uPA will not inhibit the assay initiated by active uPA.

Pre-incubation of pro-uPA with mAb-112, mAb-12E6B10 or mAb-PUK inhibited the generation of plasmin (Figure 1). Plasminogen activation catalysed directly by active two-chain uPA was also reduced when uPA was pre-incubated with mAb-112 or mAb-12E6B10, but not with mAb-PUK. However, whereas mAb-12E6B10 was equally effective in inhibiting plasmin generation in assays initiated by pro-uPA or active uPA, much higher concentrations of mAb-112 were needed to inhibit active uPA (Figure 1A, 1B, 1E and 1F). At high concentrations, mAb-101 showed a small stimulating effect when pro-uPA was the initiator. Stimulation of plasminogen activation by anti-uPA antibodies has previously been reported and presumed to be due to formation of a ternary complex between antibody, uPA and plasminogen, antibody-plasminogen binding mediated by binding of C-terminal lysine residue of the antibody to the kringles of plasminogen [32]. In contrast, no inhibition of plasminogen activation was observed using a control antibody, anti-PAI-1 mAb-2, regardless of whether the reaction was initiated by pro-uPA or uPA (Figure 1G, 1H, 1I and 1J).

In view of the fact that mAb-PUK was only effective when pro-uPA was the initiator, we evaluated the effect of this antibody on the activation of pro-uPA using a more direct approach, in which generation was active uPA from pro-uPA was measured with a chromogenic substrate. mAb-PUK caused an almost complete inhibition of pro-uPA activation by both plasmin and matriptase (Figure 2). We previously reported the same findings in the case of mAb-112 [15]. Furthermore, neither mAb-PUK nor mAb-12E6B10 showed any direct inhibitory activity towards S-2444 cleavage by either pro-uPA or active uPA (data not shown). In contrast, we previously reported that mAb-112 is a non-competitive inhibitor of S-2444 cleavage by uPA with a K_i similar to the K_D for mAb-112 binding to active two-chain uPA [15].

Effects of the monoclonal antibodies on cell surface-associated plasminogen activation

Cell surface-associated plasminogen activation catalysed by uPAR-bound uPA was assessed using U937 cells, which express high levels of uPAR. By including α_2-antiplasmin in the assay, the plasmin activity is restricted to the cell surface where plasmin is protected from inhibition by this serpin. The same inhibitory functionalities that were found in the coupled assay without cells were recapitulated in the cell-dependent assay (Figure 3). Thus, the antibodies were also able to distinguish between pro-uPA and active uPA in a cell-based setting. The IC_{50} values of the inhibition of plasminogen activation were calculated from plots of the relative fluorescence development after incubation for 60 min. When pro-uPA was incubated with mAb-PUK or uPA was incubated with mAb-12E6B10 or mAb-112, IC_{50} values of ~ 10 nM were found. When pro-uPA was incubated with mAb-112, an IC_{50} value of ~ 1 nM was found. At high concentrations, mAb-101 displayed an inhibitory effect on plasminogen activation at the cell surface. Given the fact that mAb-101 has a K_D for

binding to pro-uPA and uPA, respectively, similar to those for mAb-PUK and mAb-12E6B10, this effect is likely to be non-specific.

The effects of the monoclonal antibodies on *in vitro* and *in vivo* cell invasion

To address the potential of the antibodies for interfering with uPA-dependent cell invasion, two different invasion assays were employed. The first was the Matrigel invasion assay, where the cells must proteolytically degrade basement membrane proteins in order to cross an extracellular matrix barrier. The second *in vitro* assay was a three-dimensional invasion model, where cancer cells are incorporated into a collagen droplet and allowed to escape into surrounding matrix composed of collagen and fibrin. In these invasion assays, we used a highly disseminating cell variant of the PC-3 prostate carcinoma, *i.e*., PC-hi/diss, dissemination of which in the chicken embryo was shown to be dependent on the uPA-plasmin system [26]. We now found that mAb-PUK, mAb-12E6B10, and mAb-112 were all able to significantly inhibit cell invasion in the Matrigel assay by 35–40% (Figure 4A). Also in the cell escape assay, all three monoclonal antibodies inhibited tumour cell invasion. but mAb-112 was a more efficient inhibitor than the two other antibodies (Figure 4B).

We then analysed the capacity of the monoclonal antibodies to inhibit dissemination of PC-hi/diss cells *in vivo* using the chicken embryo chorioallantoic membrane (CAM) model system. mAb-112 reduced the level of dissemination of PC-hi/diss cells to 40% of control (Figure 4D), but other antibodies were without effect (Figure 4A, 4B and 4D). None of the antibodies affected *in vivo* tumour growth (Figure 4C),

Detection of uPA and pro-uPA on the surface of cultured cells by the use of the monoclonal antibodies

The ability of the antibodies to bind pro-uPA or uPA prebound to uPAR on the surface of a CM5 sensor chip was tested using surface plasmon resonance analysis. mAb-101, mAb-112 and mAb-12E6B10 showed unaltered binding to pro-uPA and uPA prebound to uPAR. Surprisingly, mAb-PUK showed a more than 10-fold reduced binding to uPAR-bound pro-uPA in this analysis.

Subsequently, the capability of mAb-112 and mAb-12E6B10 to bind to cell surface-associated pro-uPA or active uPA was tested by immunofluorescence analysis of non-permeabilized PC-hi/diss cells. When the cells were grown in serum-free medium, uPA was primarily present in the pro-form, as indicated by Western blot analysis of the conditioned medium (Figure 5A). Correspondingly, under serum-free conditions, PC-hi/diss cells could be stained with mAb-112 (58.9 ± 41.7 % positively stained cells), which preferentially binds to the pro-uPA, whereas no fluorescence was detected with mAb-12E6B10, which exclusively recognizes active uPA (Figure 5B). In contrast, when the cells were grown in the presence of 0.1% chicken serum, which allows for the plasmin-mediated generation of two-chain active uPA (Figure 5A), the surface of PC-hi/diss cells was could be stained with mAb-12E6B10 (24.1 ± 8.3 % positively stained cells), whereas very little staining was observed with mAb-112 (4.7 ± 4.3 % positively stained cells) (Figure 5B). Both the processing of pro-uPA to two-chain uPA and the positive cell surface staining with mAb-12E6B10 were abrogated if PC-hi/diss cells were grown in 0.1% chicken serum, but in

the presence of aprotinin, a potent inhibitor of plasmin (2.1 ± 3.6 % positively stained cells with mAb-12E6B10), whereas the cells under these conditions could be stained with mAb-112 (76.2 ± 21.2 % positively stained cells) (Figure 5A and 5B). mAb-PUK was also tested in the staining analyses, but its use did not result in positive staining which is in agreement with the much reduced binding of mAb-PUK to uPAR-bound pro-uPA (data not shown). As controls, mAb 29-7, binding CD44, was used as a positive control and mouse IgG antibody as a negative control.

Mechanisms of inhibition of pro-uPA activation

The results shown above indicated that the pro-uPA selective antibodies mAb-112 and mAb-PUK are able to inhibit pro-uPA activation. We now wished to characterise the mechanism behind this effect. To directly evaluate whether these antibodies influenced the rate of cleavage of single-chain pro-uPA into two-chain active uPA, pro-uPA was incubated with plasmin in the presence or absence of the antibodies for different periods of time before being subjected to SDS-PAGE and immunoblotting analysis. In the presence of excess mAb-PUK, the plasmin-catalysed proteolytic cleavage of pro-uPA was significantly delayed, in agreement with the above described inhibition of plasminogen activation (Figure 6). We previously reported the same findings in the case of mAb-112 [15].

Effect of the antibodies interfere on the interaction between PAI-1 and pro-uPA or uPA

The very slow reaction between pro-uPA and PAI-1 can be followed by the formation of a covalent complex of M_r ~ 100,000 in SDS-PAGE. In agreement with previously published data, mAb-112 completely blocked the complex formation [17]. mAb-PUK caused an approximately 3.5-fold reduction of the pseudo-first-order rate constant (k_{obs}) (Figure 7). mAb-12E6B10 was previously shown to strongly delay the reaction between active uPA and PAI-1 [21]. Conversely, mAb-101 did not inhibit the reaction of PAI-1 with neither pro-uPA nor uPA and (Figure 7 and data not shown).

We next analyzed whether the antibodies bind to preformed covalent uPA-PAI-1 or pro-uPA-PAI-1 complexes. Such complexes were therefore captured on the surface of a Biacore sensor chip by the anti-PAI-1 antibody mAb-7, which binds to the α-helix D-β-strand 2A loop of PAI-1, distant from the expected postion of uPA or pro-uPA in the complexes [33]. It was found that only mAb-101 was able to bind measurably to the covalent complexes between uPA and PAI-1 or pro-uPA and PAI-1, with K_D-values equal to that for the free proteins, whereas the other antibodies showed no measurable binding to the complexes (data not shown).

Localisation of the epitopes for the antibodies

We mapped the epitopes for mAb-101, mAb-12E6B10 and mAb-PUK by alanine-scanning-mutagenesis with uPA variants expressed in HEK293 cells. The epitope for the pro-uPA-selective antibody mAb-PUK was analysed with conditioned medium from cells cultured in the presence of aprotinin, ensuring that all uPA remained in the pro-form. The epitope for the active uPA-selective antibody mAb-12E6B10 was analysed with conditioned medium without aprotinin and treated with plasmin to ensure complete conversion to active uPA. Since mAb-112 was found to be able to compete with mAb-PUK for binding to pro-uPA

and with mAb-12E6B10 for binding to active uPA, residues in the vicinity of the epitope for mAb-112 [15] were chosen for the analysis of the epitopes for mAb-12E6B10 and mAb-PUK. Binding of both antibodies was found to be dependent on specific residues within the activation- and/or autolysis-loop in the activation domain (Table 2, Figure 8). We found that the binding of both mAb-PUK and mAb-12E6B10 (as well as mAb-112) depends on the the same three residues within the autolysis loop, namely Glu144, Tyr149, and Tyr 151. Furthermore, mAb-PUK and mAb-12E6B10 also showed reduced binding when specific residues in the activation loop were mutated. For mAb-PUK, this involved the residues Lys15, Ile16 and Ile17, and consequently, mAb-PUK proved to have an epitope spanning the peptide bond that is cleaved upon activation of pro-uPA. Mutagenesis of the buried residue Asp194 decreased the binding to to mAb-12E6B10 and mAb-112 but not to mAb-PUK. This residue changes conformation during the activation of serine protease zymogens in general as it makes a salt bridge to the new N-terminus in the two-chain form [ref],. Effects of muating Asp194 is therefore expected to caused by changes of the conformation of the activation domain.

MAb-101 was found to bind away from the activation domain, involving residues in the 110-loop, explaining the inability of this antibody to interfere with events involving the activation domain of uPA (Table 2, Figure 8).

DISCUSSION

Previously, a number of monoclonal anti-uPA antibodies inhibiting the enzyme activity have been described in the literature. The first monoclonal anti-uPA antibody, selected by its ability to inhibit uPA-catalysed plasminogen activation was reported in 1982 [34], but the epitope or mechanism of action of this antibody was never reported. Later, a series of inhibitory antibodies were found to have epitopes in the 37- and/or 60-loop of uPA and to inhibit uPA-catalysed plasminogen activation by steric hindrance [18]. These antibodies bind pro-uPA and active uPA equally well, but have a slightly reduced affinity to the uPA-PAI-1 complex. Recently, an antibody inhibiting mouse uPA-catalysed plasminogen activation was reported to be able to impair uPA-mediated hepatic fibrinolysis and delay skin wound healing in tPA-deficient mice. However, the epitope and detailed mode of inhibition has not been reported [35];[36].

We here report further data on the inhibitory mechanisms of three previously developed anti-human uPA antibodies, mAb-112, mAb-PUK, and mAb-12E6B10, each having differential binding affinity to single-chain pro-uPA and two-chain active uPA. Furthermore, a fourth antibody, mAb-101, also binding the catalytic domain of uPA but distant from the active site, is reported. This antibody binds pro-uPA, active uPA, and the uPA-PAI-1 complex equally well, yet does not inhibit pro-uPA activation or enzyme activity of uPA and does not perturb formation of the uPA-PAI-1 complex reaction.

In this study, we placed particular emphasis on characterising the epitopes and inhibitory mechanisms for two conformation-specific antibodies, mAb-PUK and mAb-12E6B10, in comparison to a previously partially characterised pro-uPA-specific antibody, mAb-112 [15]. The first, mAb-PUK, is a commercial antibody known to have preference for pro-uPA

over two-chain uPA. Previously reported pro-uPA-specific antibodies, generated by immunising mice with full length pro-uPA, lack a detailed functional characterisation and epitope mapping [37]. We here demonstrate that mAb-PUK is able to inhibit plasmin- and matriptase-catalysed cleavage of single-chain pro-uPA into two-chain active uPA (Figure 9). Also, we show that it has an epitope spanning the cleavage site at Lys15-Ile16 as well as additional contacts within the autolysis loop. Therefore, it apparently inhibits pro-uPA cleavage by blocking the access of activating proteases to this peptide bond. The ability to inhibit pro-uPA cleavage is common to mAb-PUK and mAb-112, in good agreement with their overlapping epitopes. Nevertheless, although the epitopes for the two antibodies are overlapping, they are clearly different. Thus, K15, Ile16, and Ile17 are not part of the epitope for mAb-112 [15]. This difference in the epitopes is in good agreement with the fact that mAb-112 inhibits the conformational change following cleavage [15], while mAb-PUK can no longer bind after cleavage has occured.

mAb-12E6B10, previously shown to be selective for two-chain uPA over pro-uPA [21], was found to bind an epitope comprising the autolysis loop and activation loop. Thus, mAb-12E6B10 has an epitope different from previously characterised antibodies inhibiting the activity of two-chain uPA. In spite of the overlap of the epitopes for mAb-12E6B10 and mAb-112, they do not inhibit two-chain uPA by the same mechanism. In contrast to mAb-112, mAb-12E6B10 only inhibits the plasminogen activation activity of uPA, and not catalysis of hydrolysis of the small chromogenic substrate S-2444 (data not shown), showing that mAb-12E6B10 does not induce a conformational change in the active site, but rather inhibits plasminogen activation by sterically interfering with access of plasminogen to uPA (Figure 9). Interestingly, it has previously been reported that the autolysis loop of tPA forms an exosite for plasminogen [38]. The localization of the epitope for mAb-12E6B10 and the ability to inhibit plasminogen activation by a steric mechanism is therefore in agreement with the hypothesis that the autolysis loop of also uPA can make an exosite interaction with plasminogen. Thus, targeting the autolysis-loop represents a new way of inhibiting plasminogen activation by uPA. The number of residues implicated in the epitope of mAb-12E6B10 is much larger than seen for mAb-112 and mAb-PUK. This finding agrees well with the fact that the binding of mAb-12E6B10 is extremely sensitive to conformational changes, rather than the result of all residues being directly implicated in binding. Asp194 is buried in the activation domain and directly associated with the catalytic site. Mutating this residue caused a significantly decreased binding of mAb-112 as well as of mAb-12E6B10, again demonstrating the sensitivity of these antibodies to conformational changes. mAb-PUK, on the other hand, was unaffected by this mutation and the action of this antibody therefore seems to be more dependent on the protection of the K15-I16 bond rather than on the conformation of the autolysis-loop.

The three-dimensional structure of pro-uPA remains to be reported, but from the three-dimensional structures of trypsinogen and trypsin, the autolysis loop is part of the activation domain which changes conformation after cleavage of trypsinogen [1]. The localization of the epitopes in the autolysis loop is therefore in good agreement with the preference of these antibodies for either pro-uPA or active uPA. Even some specific amino acid residues, *i.e.*, Glu144, Tyr149 and Tyr151, are part of the epitopes for all three antibodies. Given the

differential reactivities of the antibodies towards the different forms of u-PA, this observation indicates that these residues are differently oriented in pro-uPA and u-PA, thereby providing evidence for structural changes within this loop upon zymogen activation. In previous studies, mAb-112 was shown to be a non-competetive inhibitor of active uPA cleaving a small substrate [15] and able to hinder the effect of dipeptides stimulating the activity of pro-uPA [17]. This indicates that the autolysis-loop bound by mAb-112 is restrained in a conformation that does not allow the active site to mature. Thus, mAb-112 obviously shifts the equilibrium between the pro- and the active conformation in favour of the pro-conformation. In contrast, mAb-12E6B10 and mAb-PUK are totally selective for active uPA and pro-uPA, respectively and do not seem change the equilibrium between active and inactive conformations, based on the fact that neither of them induced or inhibited the ability of pro-uPA or uPA to catalyse hydrolysis of S-2444.

The ability of mAb-PUK, mAb-12E6B10 and mAb-112 to inhibit formation of the pro-uPA-PAI-1 complex or active uPA-PAI-1 complex and inability of the antibodies to bind to the preformed complexes is likely to be caused by competition with PAI-1 for the same binding site on pro-uPA and uPA. The recently determined three-dimensional structure of a Michaelis complex between uPA and PAI-1, representing the initial encounter between inhibitor and enzyme, shows that the autolysis loop is engaged in hydrogen bonding interactions with PAI-1 [39]. Occupation of the autolysis loop by an antibody would therefore be incompatible with formation of this complex (Figure 10A). The stable covalent complex between uPA and PAI-1 has not yet been reported. However, based on structures of homologous protease-serpin complexes, a model of the complex can be built (Figure 10B). The model shows that the autolysis loop is close to the body of the serpin and unlikely to be accessible to an antibody. Importantly, the two tyrosine residues implicated in all three epitopes are within a distance of a few angstroms from PAI-1.

A number of inhibitors of the proteolytic activity of uPA have been developed, including small organochemical molecules, peptides, and monoclonal antibodies, both with a view to their use for elucidating the pathophysiological functions of uPAs various molecular interactions and to generate leads for drug development (for a review see [40]). The most specific inhibitors to date appear to be those derived from antibodies and peptidylic inhibitors, which utilize binding sites involving surface loops of uPA and extended exosite interactions that drive selectivity and specificity. A strategy targeting regulatory regions outside the catalytic site, *i.e.* those regions related to pro-enzyme activation, likely provide unique inhibitor-protease interaction surfaces and is, thus, expected to enhance the chances of engineering high inhibitor specificity. The conformational antibodies characterized in this study were evaluated for their ability to inhibit cell invasion in two different invasion assays. Although simplified systems, these assays partially recapitulate the escape of cancer cells from a primary tumour and their invasion into the surrounding stroma. All three antibodies proved equally able to inhibit cancer cell invasion in the Matrigel assay. However, in a more complex *in vitro* setting, namely tumour cell escape into fibrin-enriched 3-D collagen, mAb-112 was the most efficient in the inhibition of cancer cell invasion. Furthermore, in the *in vivo* setting in the chick embryo CAM model, only mAb-112 proved to be an effective inhibitor of cancer cell dissemination. The affinity of mAb-112 to pro-uPA was

approximately 10-fold higher compared to the affinity of mAb-PUK and mAb-12E6B10 to pro-uPA and uPA, respectively. The same difference was observed for the inhibition of plasminogen activation on the cell surface of U937 cells, where a 10-fold lower IC_{50}-value for mAb-112 was observed when pro-uPA initiated the reaction. Therefore, the reason for the higher potency of mAb-112 in the *in vivo* inhibition of cancer cell dissemination is probably the result of a higher affinity and/or the bi-functional inhibitory mechanism displayed by mAb-112 (Figure 9).

The relative amounts of active two-chain uPA and inactive pro-uPA in the tumour microenvironment could have great impact on tumour growth and metastasis, but, to the best of our knowledge, differential detection of each of these two forms directly on the cell surface has not been carried out previously. Therefore, the selective ability of the antibodies to recognize pro-uPA or uPA was exploited to detect cell surface-bound pro-uPA or uPA. In agreement with the presence of either pro-uPA or uPA in the culture, the PC-hi/diss cells were positively stained either with mAb-112 or mAb-12E6B10, respectively. Therefore, this pair of mAbs might represent a new tool for evaluating the activation status of urokinase-type plasminogen activator in the tumour microenvironment and to study whether pro-uPA or active uPA or both are relevant targets.

In conclusion, a functional characterisation of conformation-specific monoclonal antibodies demonstrates that the autolysis-loop of urokinase-type plasminogen activator is highly implicated in the conformational changes that form a mature active site when pro-uPA is converted to active uPA. The efficacy of targeting plasminogen activation by interfering with regions on uPA outside the highly conserved catalytic site has been shown herein to be a feasible way of hindering cancer cell invasion and dissemination *in vivo*. Finally, the conformation-specific antibodies proved to be able to discriminate between pro-uPA versus uPA on the surface of live cells.

ACKNOWLEDGMENT

This work was supported by grants from the Danish Cancer Society (DP 07043, DP 08001); the Danish National Research Foundation (26-331-6); National Natural Science Foundation of China (30811130467, 30973567, 30770429); the Danish Research Agency (272-06-0518); and the Novo Nordisk Foundation (R114-A11382).

Abbreviations used

CAM	chorioallantoic membrane
mAb	monoclonal antibody
PAI-1	plasminogen activator inhibitor-1
PMSF	phenylmethylsulfonyl fluoride
S-2444	H-D-Glu-Gly-Arg-p-nitroanilide
SPR	surface plasmon resonance
TIU	trypsin inhibitory unit
uPA	urokinase-type plasminogen activator

VLK-AMC	H-D-Val-Leu-Lys-7-amido-4-methylcoumarine
wt	wild type

REFERENCES

1. Bode W, Schwager P, Huber R. The transition of bovine trypsinogen to a trypsin-like state upon strong ligand binding. The refined crystal structures of the bovine trypsinogen-pancreatic trypsin inhibitor complex and of its ternary complex with Ile-Val at 1.9 A resolution. J Mol Biol. 1978; 118:99–112. [PubMed: 625059]
2. Hedstrom L. Serine protease mechanism and specificity. Chem Rev. 2002; 102:4501–4524. [PubMed: 12475199]
3. Ye S, Goldsmith EJ. Serpins and other covalent protease inhibitors. Curr Opin Struct Biol. 2001; 11:740–745. [PubMed: 11751056]
4. Huntington JA. Shape-shifting serpins--advantages of a mobile mechanism. Trends Biochem Sci. 2006; 31:427–435. [PubMed: 16820297]
5. Dupont DM, Madsen JB, Kristensen T, Bodker JS, Blouse GE, Wind T, Andreasen PA. Biochemical properties of plasminogen activator inhibitor-1. Front Biosci. 2009; 14:1337–1361.
6. Dano K, Andreasen PA, Grondahl-Hansen J, Kristensen P, Nielsen LS, Skriver L. Plasminogen activators, tissue degradation, and cancer. Adv Cancer Res. 1985; 44:139–266. [PubMed: 2930999]
7. Andreasen PA, Kjoller L, Christensen L, Duffy MJ. The urokinase-type plasminogen activator system in cancer metastasis: a review. Int J Cancer. 1997; 72:1–22. [PubMed: 9212216]
8. Andreasen PA, Egelund R, Petersen HH. The plasminogen activation system in tumor growth, invasion, and metastasis. Cell Mol Life Sci. 2000; 57:25–40. [PubMed: 10949579]
9. List K, Jensen ON, Bugge TH, Lund LR, Ploug M, Dano K, Behrendt N. Plasminogen-independent initiation of the pro-urokinase activation cascade in vivo. Activation of pro-urokinase by glandular kallikrein (mGK-6) in plasminogen-deficient mice. Biochemistry. 2000; 39:508–515. [PubMed: 10642175]
10. Kilpatrick LM, Harris RL, Owen KA, Bass R, Ghorayeb C, Bar-Or A, Ellis V. Initiation of plasminogen activation on the surface of monocytes expressing the type II transmembrane serine protease matriptase. Blood. 2006; 108:2616–2623. [PubMed: 16794252]
11. Moran P, Li W, Fan B, Vij R, Eigenbrot C, Kirchhofer D. Pro-urokinase-type plasminogen activator is a substrate for hepsin. J Biol Chem. 2006; 281:30439–30446. [PubMed: 16908524]
12. Dickinson CD, Shobe J, Ruf W. Influence of cofactor binding and active site occupancy on the conformation of the macromolecular substrate exosite of factor VIIa. J Mol Biol. 1998; 277:959–971. [PubMed: 9545384]
13. Shobe J, Dickinson CD, Ruf W. Regulation of the catalytic function of coagulation factor VIIa by a conformational linkage of surface residue Glu 154 to the active site. Biochemistry. 1999; 38:2745–2751. [PubMed: 10052945]
14. Ganesan R, Eigenbrot C, Wu Y, Liang WC, Shia S, Lipari MT, Kirchhofer D. Unraveling the allosteric mechanism of serine protease inhibition by an antibody. Structure. 2009; 17:1614–1624. [PubMed: 20004165]
15. Blouse GE, Botkjaer KA, Deryugina E, Byszuk AA, Jensen JM, Mortensen KK, Quigley JP, Andreasen PA. A novel mode of intervention with serine protease activity: targeting zymogen activation. J Biol Chem. 2009; 284:4647–4657. [PubMed: 19047064]
16. Egelund R, Petersen TE, Andreasen PA. A serpin-induced extensive proteolytic susceptibility of urokinase-type plasminogen activator implicates distortion of the proteinase substrate-binding pocket and oxyanion hole in the serpin inhibitory mechanism. Eur. J. Biochem. 2001; 268:673–685. [PubMed: 11168406]
17. Botkjaer KA, Byszuk AA, Andersen LM, Christensen A, Andreasen PA, Blouse GE. Nonproteolytic induction of catalytic activity into the single-chain form of urokinase-type plasminogen activator by dipeptides. Biochemistry. 2009; 48:9606–9617. [PubMed: 19705874]

18. Petersen HH, Hansen M, Schousboe SL, Andreasen PA. Localization of epitopes for monoclonal antibodies to urokinase-type plasminogen activator: relationship between epitope localization and effects of antibodies on molecular interactions of the enzyme. Eur. J. Biochem. 2001; 268:4430–4439. [PubMed: 11502203]
19. Dupont DM, Blouse GE, Hansen M, Mathiasen L, Kjelgaard S, Jensen JK, Christensen A, Gils A, Declerck PJ, Andreasen PA, Wind T. Evidence for a pre-latent form of the serpin plasminogen activator inhibitor-1 with a detached beta-strand 1C. J Biol Chem. 2006; 281:36071–36081. [PubMed: 17018527]
20. Wind T, Jensen JK, Dupont DM, Kulig P, Andreasen PA. Mutational analysis of plasminogen activator inhibitor-1. Eur J Biochem. 2003; 270:1680–1688. [PubMed: 12694181]
21. Declerck PJ, Lijnen HR, Verstreken M, Moreau H, Collen D. A monoclonal antibody specific for two-chain urokinase-type plasminogen activator. Application to the study of the mechanism of clot lysis with single-chain urokinase-type plasminogen activator in plasma. Blood. 1990; 75:1794–1800. [PubMed: 1691934]
22. Jespersen MH, Jensen J, Rasmussen LH, Ejlersen E, Moller-Petersen J, Sperling-Petersen HU. The reference range for complexed alpha 2-macroglobulin human plasma: development of a new enzyme linked in immunosorbent assay (ELISA) for quantitation of complexed alpha 2-macroglobulin. Scand. J. Clin. Lab. Invest. 1993; 53:639–648.
23. Knoop A, Andreasen PA, Andersen JA, Hansen S, Laenkholm AV, Simonsen AC, Andersen J, Overgaard J, Rose C. Prognostic significance of urokinase-type plasminogen activator and plasminogen activator inhibitor-1 in primary breast cancer. Br. J. Cancer. 1998; 77:932–940. [PubMed: 9528837]
24. Nielsen LS, Andreasen PA, Grondahl-Hansen J, Huang JY, Kristensen P, Dano K. Monoclonal antibodies to human 54,000 molecular weight plasminogen activator inhibitor from fibrosarcoma cells--inhibitor neutralization and one-step affinity purification. Thromb. Haemost. 1986; 55:206–212. [PubMed: 3520936]
25. Gils A, Pedersen KE, Skottrup P, Christensen A, Naessens D, Deinum J, Enghild JJ, Declerck PJ, Andreasen PA. Biochemical importance of glycosylation of plasminogen activator inhibitor-1. Thromb Haemost. 2003; 90:206–217. [PubMed: 12888867]
26. Conn EM, Botkjaer KA, Kupriyanova TA, Andreasen PA, Deryugina EI, Quigley JP. Comparative analysis of metastasis variants derived from human prostate carcinoma cells: roles in intravasation of VEGF-mediated angiogenesis and uPA-mediated invasion. Am J Pathol. 2009; 175:1638–1652. [PubMed: 19729488]
27. Lund LR, Georg B, Nielsen LS, Mayer M, Dano K, Andreasen PA. Plasminogen activator inhibitor type 1: cell-specific and differentiation-induced expression and regulation in human cell lines, as determined by enzyme-linked immunosorbent assay. Mol Cell Endocrinol. 1988; 60:43–53. [PubMed: 3265112]
28. Rasband, WS. Bethesda, Maryland, USA: U.S. National Institute of Health; 1997–2005. ImageJ. http://rsb.info.nih.gov/ij/.
29. Skriver L, Nielsen LS, Stephens R, Dano K. Plasminogen activator released as inactive proenzyme from murine cells transformed by sarcoma virus. Eur J Biochem. 1982; 124:409–414. [PubMed: 6284507]
30. Nielsen LS, Hansen JG, Skriver L, Wilson EL, Kaltoft K, Zeuthen J, Dano K. Purification of zymogen to plasminogen activator from human glioblastoma cells by affinity chromatography with monoclonal antibody. Biochemistry. 1982; 21:6410–6415. [PubMed: 6891264]
31. Behrendt N, List K, Andreasen PA, Dano K. The pro-urokinase plasminogen-activation system in the presence of serpin-type inhibitors and the urokinase receptor: rescue of activity through reciprocal pro-enzyme activation. Biochem J. 2003; 371:277–287. [PubMed: 12534347]
32. Ellis V, Dano K. Potentiation of plasminogen activation by an anti-urokinase monoclonal antibody due to ternary complex formation. A mechanistic model for receptor-mediated plasminogen activation. J Biol Chem. 1993; 268:4806–4813. [PubMed: 8444857]
33. Mathiasen L, Dupont DM, Christensen A, Blouse GE, Jensen JK, Gils A, Declerck PJ, Wind T, Andreasen PA. A peptide accelerating the conversion of plasminogen activator inhibitor-1 to an inactive latent state. Mol Pharmacol. 2008; 74:641–653. [PubMed: 18559377]

34. Kaltoft K, Nielsen LS, Zeuthen J, Dano K. Monoclonal antibody that specifically inhibits a human Mr 52,000 plasminogen-activating enzyme. Proc Natl Acad Sci U S A. 1982; 79:3720–3723. [PubMed: 6808514]

35. Lund IK, Jogi A, Rono B, Rasch MG, Lund LR, Almholt K, Gardsvoll H, Behrendt N, Romer J, Hoyer-Hansen G. Antibody-mediated targeting of the urokinase-type plasminogen activator proteolytic function neutralizes fibrinolysis in vivo. J Biol Chem. 2008; 283:32506–32515. [PubMed: 18799467]

36. Jogi A, Rono B, Lund IK, Nielsen BS, Ploug M, Hoyer-Hansen G, Romer J, Lund LR. Neutralisation of uPA with a monoclonal antibody reduces plasmin formation and delays skin wound healing in tPA-deficient mice. PLoS One. 5:e12746. [PubMed: 20856796]

37. Scheuerlein JG, Kalies I, Gluth WP, Kalden JR. Monoclonal antibodies monospecific to single-chain urokinase-type plasminogen activator (scu-PA). Hybridoma. 1991; 10:395–399. [PubMed: 1916850]

38. Ke SH, Tachias K, Lamba D, Bode W, Madison EL. Identification of a hydrophobic exosite on tissue type plasminogen activator that modulates specificity for plasminogen. J Biol Chem. 1997; 272:1811–1816. [PubMed: 8999865]

39. Lin Z, Jiang L, Yuan C, Jensen JK, Zhang X, Luo Z, Furie BC, Furie B, Andreasen PA, Huang M. Structural basis for recognition of urokinase-type plasminogen activator by plasminogen activator inhibitor-1. J Biol Chem. 286:7027–7032. [PubMed: 21199867]

40. Stoppelli, MP.; Andersen, LM.; Votta, G.; Andreasen, PA. Engineered antagonists of uPA and PAI-1 In The Cancer Degradome. Edwards, D., editor. New York: Springer; 2008. p. 721-758.

41. The PyMOL Molecular Graphics System, Version 1.2r3pre. Schrödinger, LLC: PyMOL.

42. Zhao G, Yuan C, Wind T, Huang Z, Andreasen PA, Huang M. Structural basis of specificity of a peptidyl urokinase inhibitor, upain-1. J Struct Biol. 2007; 160:1–10. [PubMed: 17692534]

43. Bolognesi M, Gatti G, Menagatti E, Guarneri M, Marquart M, Papamokos E, Huber R. Three-dimensional structure of the complex between pancreatic secretory trypsin inhibitor (Kazal type) and trypsinogen at 1.8 A resolution. Structure solution, crystallographic refinement and preliminary structural interpretation. J Mol Biol. 1982; 162:839–868. [PubMed: 7169635]

44. Arnold K, Bordoli L, Kopp J, Schwede T. The SWISS-MODEL workspace: a web-based environment for protein structure homology modelling. Bioinformatics. 2006; 22:195–201. [PubMed: 16301204]

45. Huntington JA, Read RJ, Carrell RW. Structure of a serpin-protease complex shows inhibition by deformation. Nature. 2000; 407:923–926. [PubMed: 11057674]

46. Jensen JK, Gettins PG. High-resolution structure of the stable plasminogen activator inhibitor type-1 variant 14-1B in its proteinase-cleaved form: a new tool for detailed interaction studies and modeling. Protein Sci. 2008; 17:1844–1849. [PubMed: 18725454]

47. Spraggon G, Phillips C, Nowak UK, Ponting CP, Saunders D, Dobson CM, Stuart DI, Jones EY. The crystal structure of the catalytic domain of human urokinase-type plasminogen activator. Structure. 1995; 3:681–691. [PubMed: 8591045]

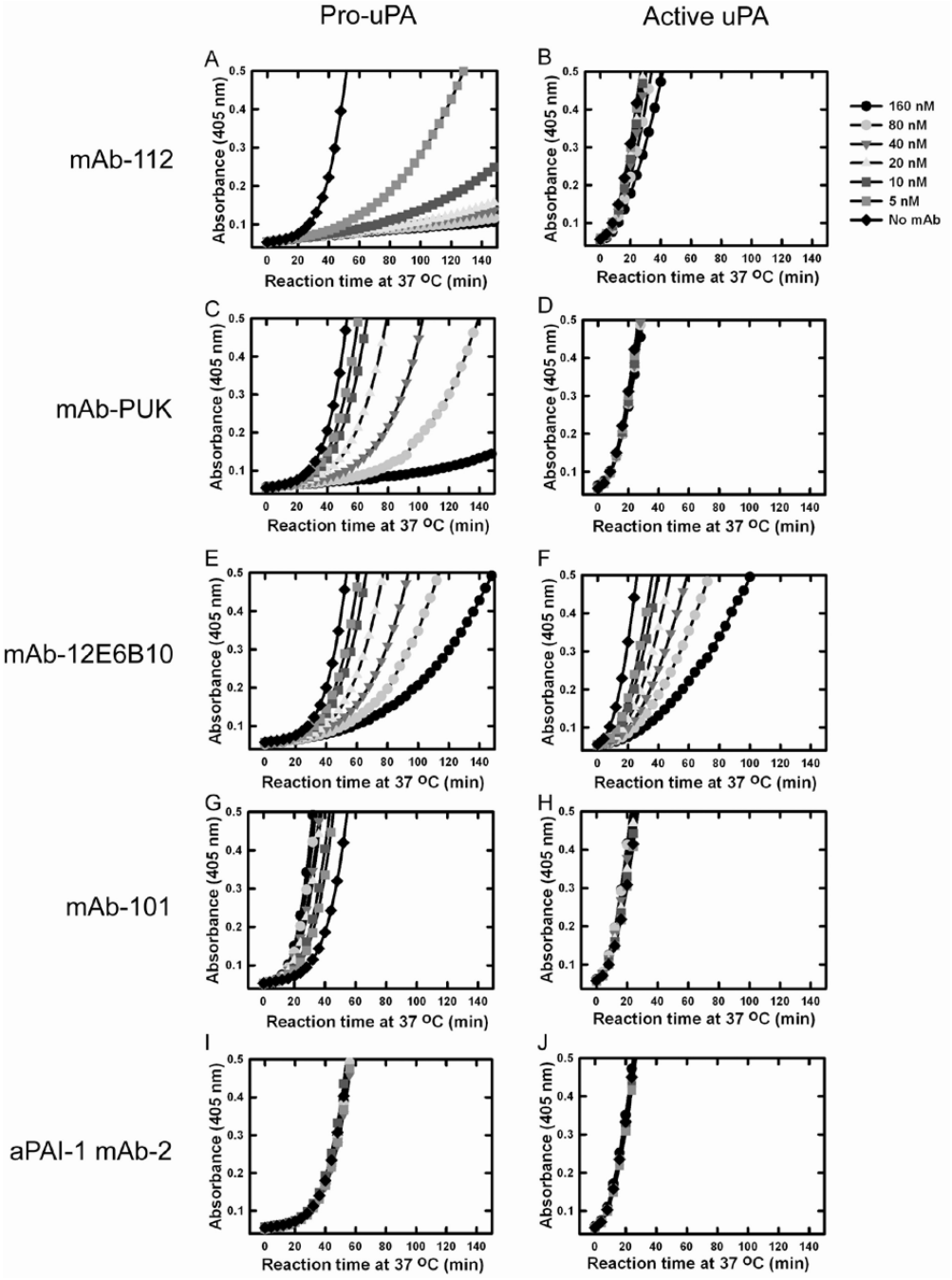

Figure 1. Functional effects of antibodies on *in vitro* plasminogen activation initiated by pro-uPA or active uPA

0.25 nM pro-uPA or 0.25 nM uPA was incubated without (*light blue dots*) antibody or with 5 nM (*pink dots*), 10 nM (*dark blue dots*), 20 nM (*yellow dots*), 40 nM (*green dots*), 80 nM (*red dots*) and 160 nM (*black dots*) of mAb-112, mAb-PUK, mAb-12E6B10, mAb-101 or anti-PAI-1 mAb-2, as indicated. After incubation for 30 min at room temperature, plasminogen was added to 0.5 μM and S-2251 to 0.5 mM. Substrate hydrolysis was

followed at 37°C by measuring the absorbance at 405 nm. Pro-uPA or uPA was omitted in controls (*grey curves*).

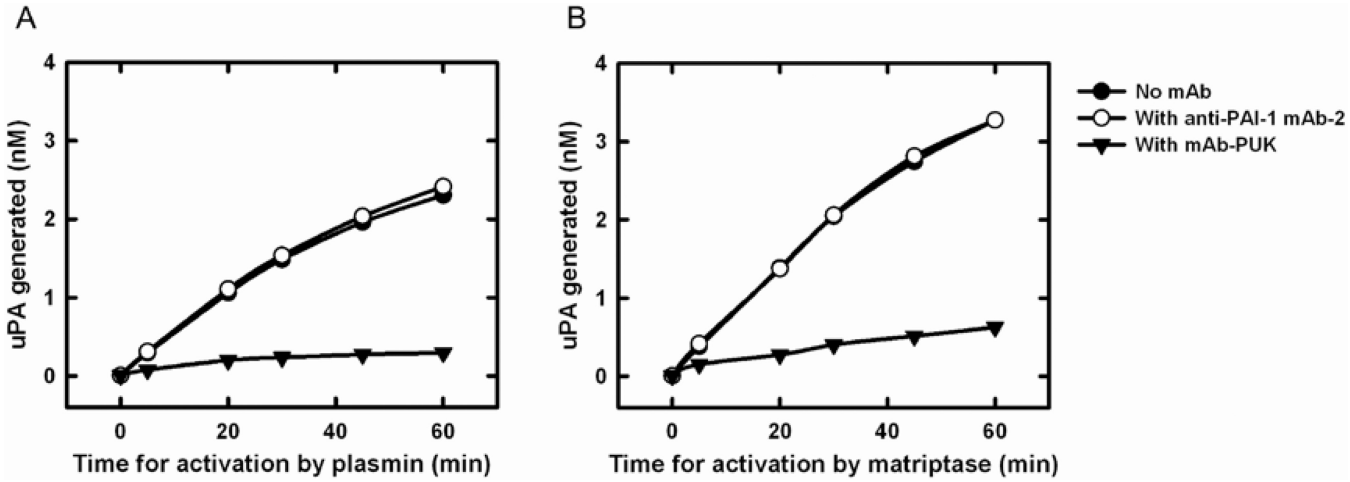

Figure 2. Effect of antibodies on the activation of pro-uPA

Ten nM pro-uPA was incubated with 100 nM mAb-PUK (*black triangles*), 100 nM anti-PAI-1 mAb-2 (*white circles*) or without antibody (*black circles*). At time zero, 0.5 nM plasmin or 5 nM matriptase was added, followed by incubation of the mixtures at room temperature for the indicated time periods. Finally, the activity of plasmin or matriptase was quenched by the addition of aprotinin to a final concentration of 1 μM. S-2444 was added to a final concentration of 0.5 mM and the amount of active uPA formed was estimated by the rate of hydrolysis and comparison to a standard curve of active two-chain uPA.

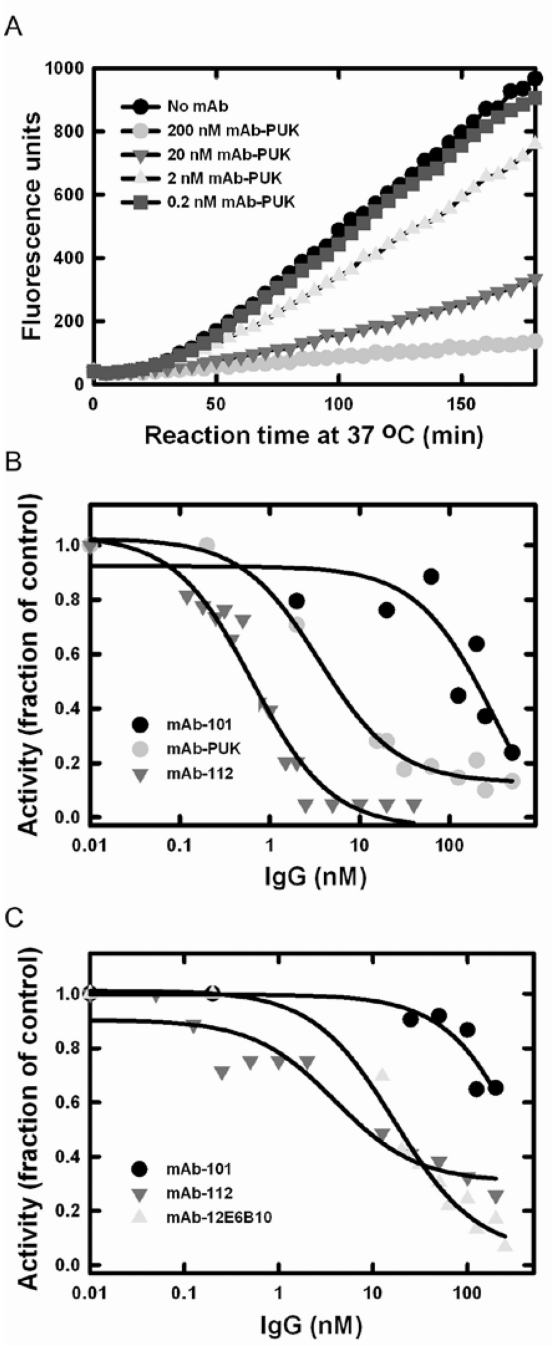

Figure 3. Effect of the antibodies on cell surface-associated plasminogen activation

U937 cells were washed with glycine-HCl, pH 3, 0.1 M NaCl to remove pro-uPA and uPA bound to the cell surface. One nM pro-uPA or uPA alone or pre-incubated with monoclonal antibodies were added to the cells together with 0.4 μM α_2-antiplasmin and 0.2 μM plasminogen. ***A***, Example of a time course experiment with pro-uPA preincubated alone (black) or with mAb-PUK at 0.2 nM (blue), 2 nM (yellow), 20 nM (green) or 200 nM (red). ***B***, IC_{50} plots of inhibition of cell surface-associated plasminogen activation by mAb-101 (black), mAb-112 (green) and mAb-PUK (red) in an assay with pro-uPA. ***C***, IC_{50} plots of

inhibition by mAb-101 (black), mAb-112 (green) and mAb-12E106B (yellow) in an assay with active uPA. All curves in ***B*** and ***C*** were fit to a hyperbolic decay equation, which provided approximate IC_{50}-values. The data shown are representative of at least three independent measurements for each condition.

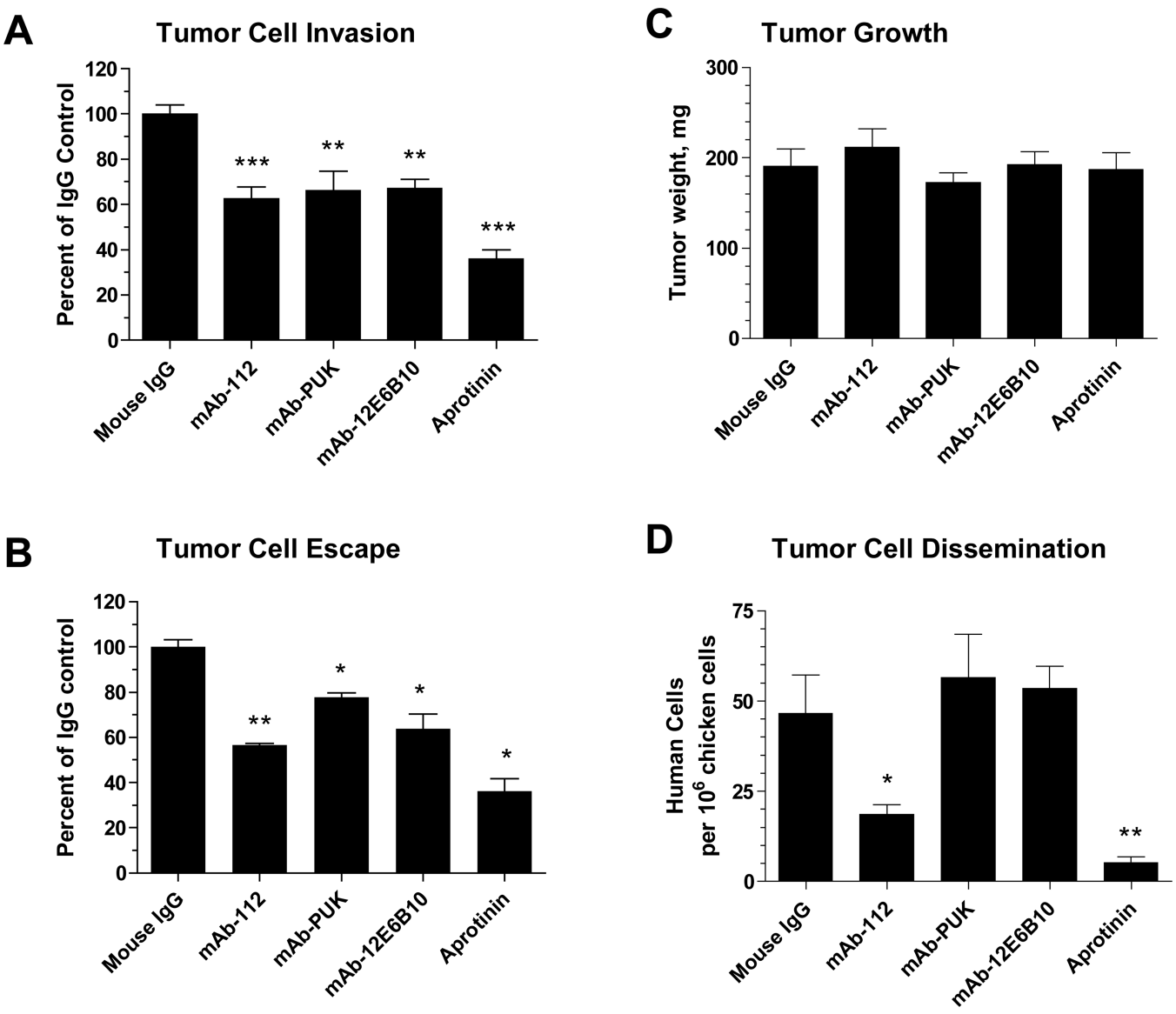

Figure 4. Inhibitory effects of antibodies on tumour cell invasion *in vitro* and dissemination *in vivo*

A, Matrigel invasion assay, in which PC-Hi/diss cells were allowed to invade the matrix barrier towards chemoattractants present in chicken embryonic fibroblast conditioned medium in the presence of 333 nM control IgG, mAb-112, mAb-PUK or mAb-12E6B10 or 0.1 TIU/ml aprotinin. The data are presented as percentage of control and are means ± SEM. ** and ***, $p<0.005$ and 0.0001, respectively. ***B***, Tumour cell escape assay, in which PC-hi/diss cells were allowed to escape the initial collagen droplet and invade a fibrin-enriched collagen matrix. Antibodies and aprotinin were incorporated in final concentrations of 167 nM and 0.1 TIU/ml, respectively. The invasion index was calculated as the number of escaped tumour cells multiplied by the distance invaded. The data are presented as percentage of control and are means ± SEM. * and **, $p<0.05$ and 0.01, respectively. ***C and D***, Spontaneous dissemination assay in chick embryos. PC-hi/diss cells were inoculated on the chorioallantoic membrane (CAM) of chicken embryos and allowed to form primary

tumours, which were excised and weighed after 7 days of growth (***C***). The numbers of disseminated PC-hi/diss cells were determined by *Alu* qPCR in the portions of the CAM distal to the site of primary tumour formation (***D***). Data are presented as numbers of human cells per 10^6 chicken cells and are means ± SEM. * and **, $p<0.05$ in one-tailed and two-tailed Student's t-test, respectively.

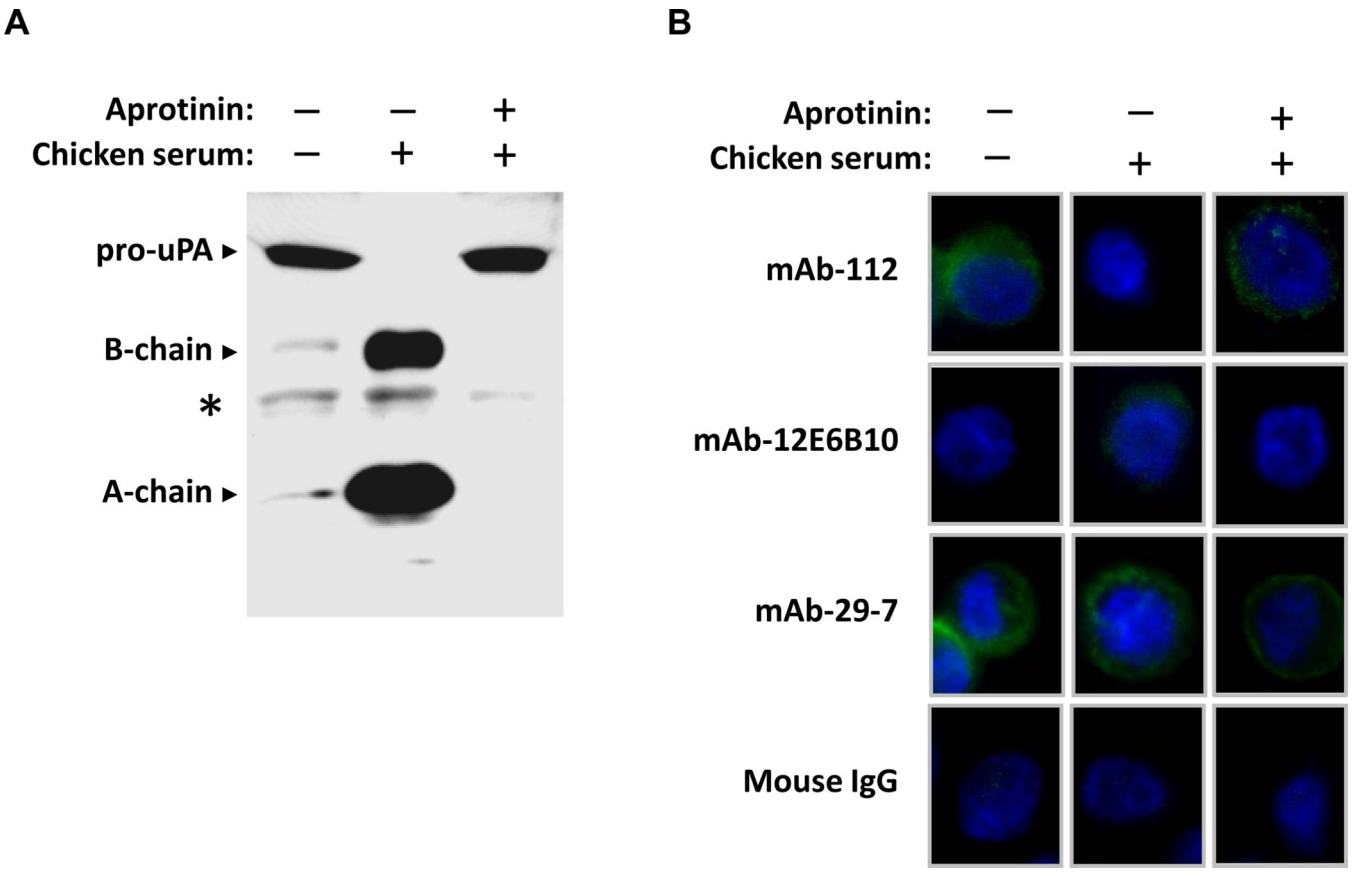

Figure 5. Conformation-sensitive antibodies used to detect pro-uPA or uPA on the cell surface

A, Western blot analysis of conditioned media from PC-hi/diss cells grown in serum-free medium or in medium supplemented with 0.1% chicken serum with or without 0.1 TUI/ml aprotinin. The proteins were separated by SDS-PAGE under reducing conditions, transferred to a membrane support and probed with a polyclonal anti-uPA antibody. Pro-uPA is detected as one band migrating at M_r ~54,000, whereas active uPA is separated into two chains, migrating at M_r~34,000 (the catalytic domain, B-chain) and M_r~20,000 (the amino-terminal fragment, A-chain). *, non-specific band. ***B***, Immunofluorescence analysis of cell surface-associated pro-uPA and active uPA. PC-hi/diss cells were grown in serum-free medium or in the presence of 0.1 % chicken serum with or without 0.1 TIU/ml aprotinin. After two days of incubation, the cells were fixed and stained without permeabilisation with mAb-112 or mAb-12E6B10. Anti-CD44 mAb-29-7 and mouse IgG were used as positive and negative controls, respectively. FITC-conjugated goat anti-mouse antibody was used to detect bound antibodies. Cell nuclei were stained with DAPI.

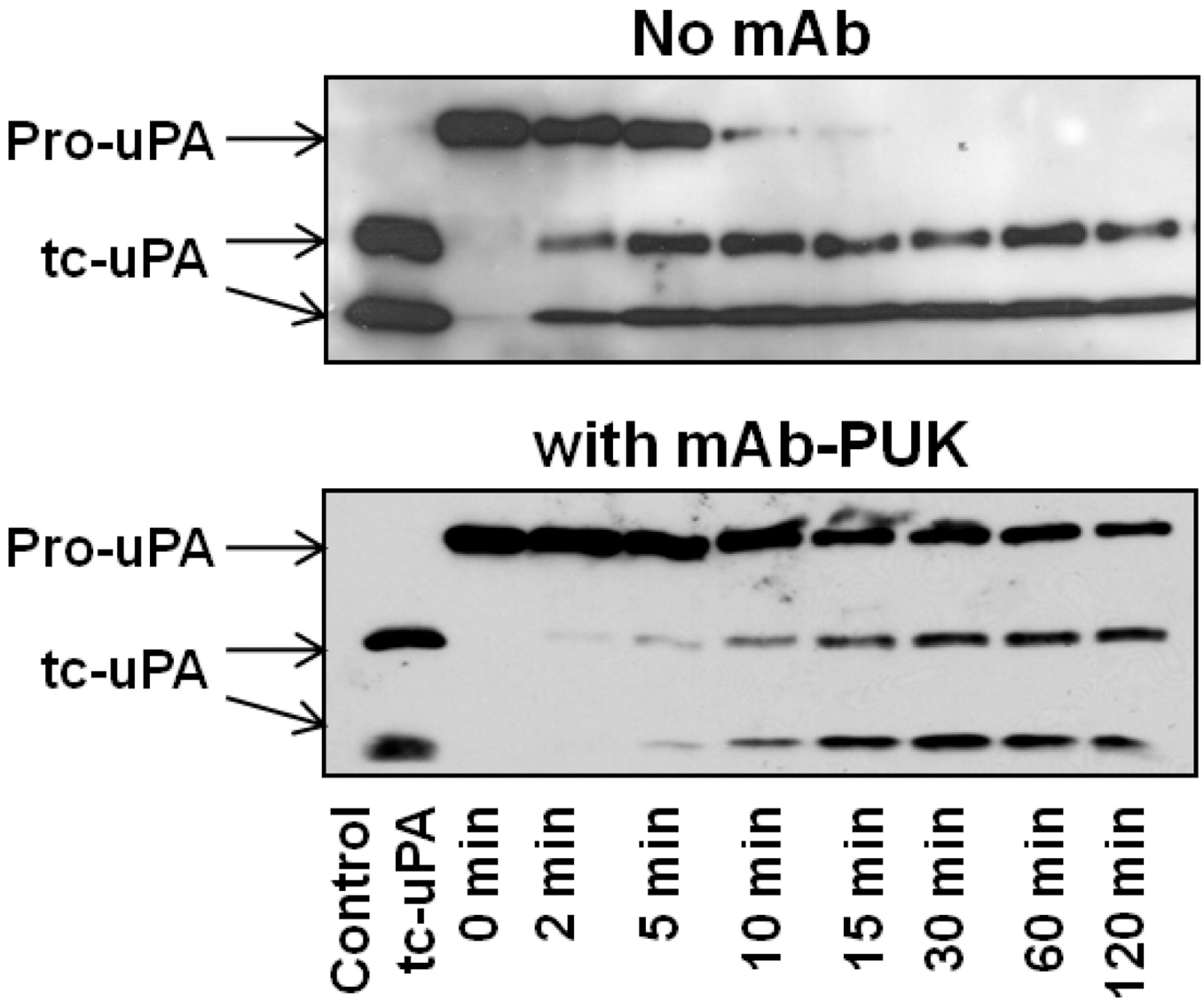

Figure 6. Effect of antibodies on plasmin-catalysed cleavage of single-chain pro-uPA

Aliquots of pro-uPA (200 nM) were incubated with plasmin (5 nM) in the absence or presence of mAb-PUK (300 nM). After the indicated incubation periods, the reaction products were analyzed by reducing SDS-PAGE and immunoblotting with a polyclonal anti-uPA antibody. Two-chain active uPA was added to lane one as a control. The cleavage by plasmin was observed as the conversion of the M_r ~54,000 band of single-chain pro-uPA to the M_r~34,000 catalytic domain and M_r~20,000 amino-terminal fragment of two-chain uPA.

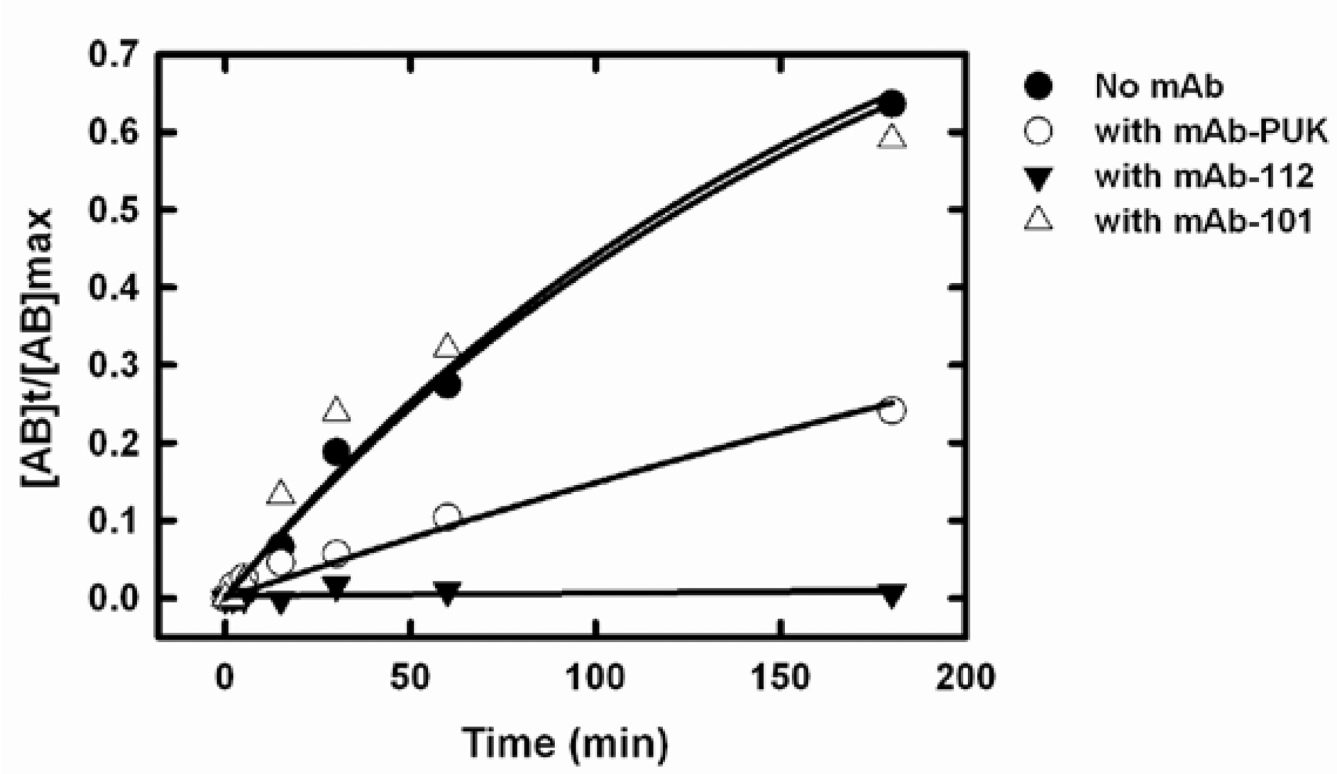

Figure 7. Time course of complex formation between single-chain uPA and PAI-1

Single-chain uPA (2 μM) was incubated with PAI-1 (3 μM) at room temperature, with or without monoclonal antibodies (4 μM). Reactions were stopped at varying time points by adding PMSF to a final concentration of 1 mM and boiling in sample buffer. The products were analyzed by SDS-PAGE and the relative densities of the bands corresponding to single-chain pro-uPA alone and the single-chain pro-uPA-PAI-1 complex were estimated by densitometric scanning of the gels. The fraction of total pro-uPA that was in complex with PAI-1 was plotted against the time of incubation in the presence of mAb-PUK (white circles), mAb-112 (black triangles), mAb-101 (white triangles) or in the absence of antibody (black circles). k_{obs} values for a monoexponential approach to steady state were calculated by fitting the data points to the equation $[AB]_t/[AB]_{max} = 1 - e^{kobs*t}$, where $[AB]_t$ is the amount of complex formed between pro-uPA and PAI-1 at time t, $[AB]_{max}$ is the maximal amount of complex that can be formed and t is the reaction time (also see Experimental procedures).

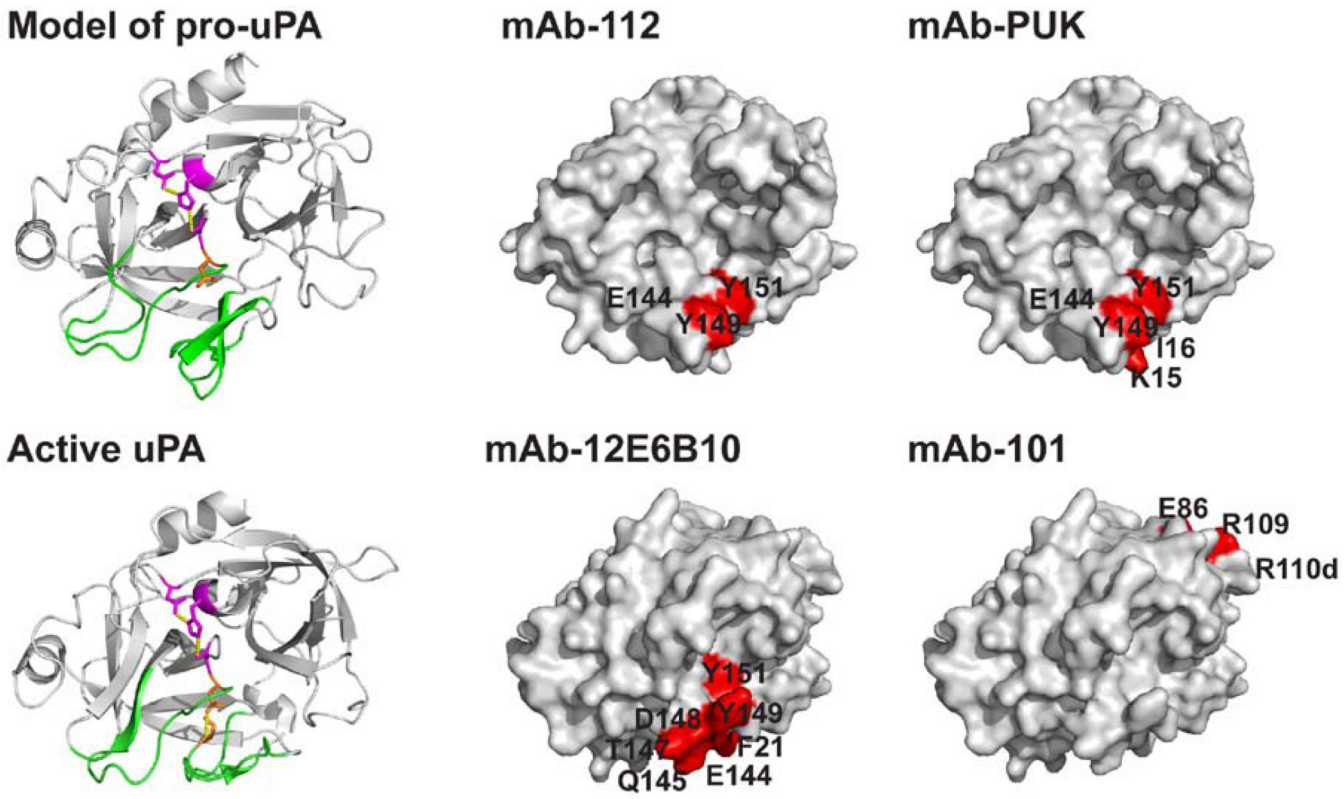

Figure 8. Models of the three-dimensional structures of uPA and pro-uPA, with the epitopes for mAb-PUK, mAb-112, mAb-12E6B10 and mAb-101

A homology model of the catalytic domain of pro-uPA build on the three-dimensional structure of trypsinogen is shown in ribbon with the activation domain (green), the catalytic triad (purple) and Ile16 (orange) highlighted. The catalytic domain of uPA is shown in ribbon with the same structural elements highlighted as in the model of pro-uPA and with the Ile16-Asp194 salt bridge in orange. The epitopes for mAb-PUK and mAb-112 are shown on a surface representation of the model for pro-uPA displayed in the same orientation as in the ribbon image. The epitopes for mAb-12E6B10 and mAb-101 are shown on a surface representation of the serine protease domain of active two-chain uPA also in the same orientation as in the ribbon image. Alanine substitution of residues depicted in red resulted in a more than 5-fold reduction in the affinity for the antibodies. These images were created in PyMol [41] on the basis of the coordinates provided in PDB entry 2NWN for two-chain active uPA [42] and 1TGS for trypsinogen [43]. The homology model of pro-uPA was made using SWISS-MODEL [44].

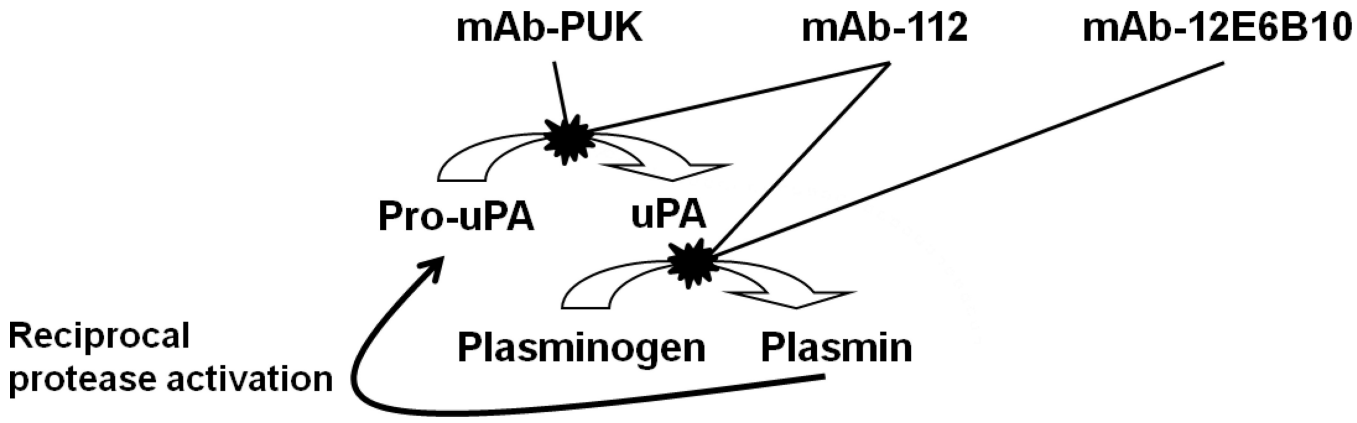

Figure 9. A schematic representation of the protease cascade showing the point of action for the inhibitory antibodies

A simplified representation of the protease cascade showing pro-uPA conversion to active uPA which subsequently activates plasminogen to plasmin. Plasmin in turn generates a reciprocal protease activation loop by producing more uPA from pro-uPA. mAb-PUK and mAb-112 blocks the cleavage of pro-uPA to two-chain active uPA. mAb-12E6B10 and mAb-112 interferes with uPA-catalysed plasminogen activation.

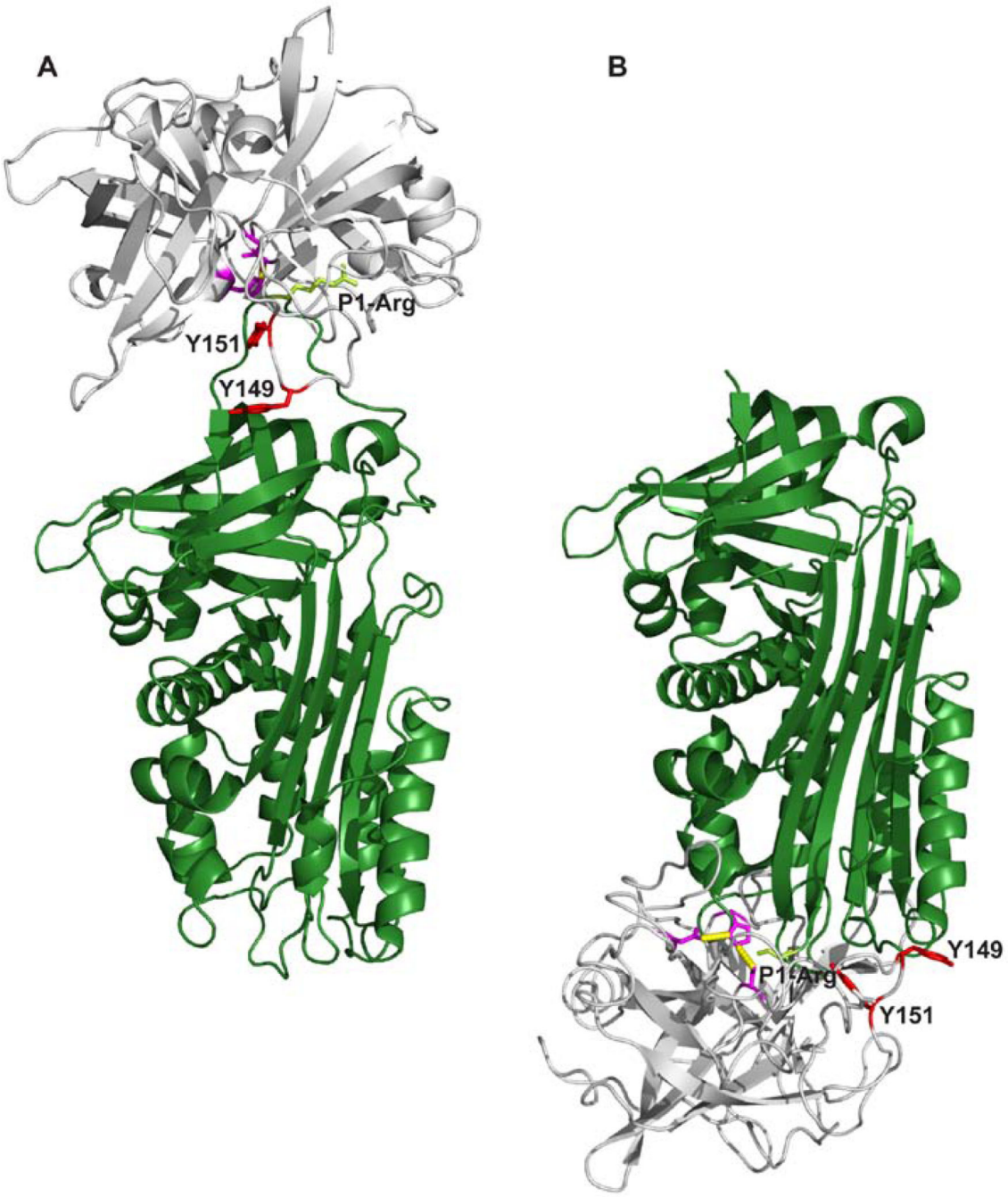

Figure 10. A model of the complexes between uPA and PAI-1

A, The Michaelis complex between uPA and PAI-1, with uPA in gray and PAI-1 in dark green [39]. The catalytic triad of uPA is coloured purble with the two tyrosine residues, Y149 and Y151, involved in the epitopes of the conformation-sensitive antibodies depicted in red. Shown in light green are the side chain of the P1-arginine residue of PAI-1. ***B***, A model of the stable uPA-PAI-1 complex build on the basis of the complex between α_1-antitrypsin and trypsin [45], with the same colour codes as in ***A***. All figures were constructed with Pymol [41] on the basis of the coordinates given in the PDB entry 3CVM for PAI-1

[46], 1LMW for two-chain active uPA [47], 1EZX for the stable covalent complex between α_1-antitrypsin and trypsin [45] and 3PB1 for the Michaelis complex between uPA and PAI-1[39].

Table 1

Kinetic analysis of the binding of antibodies to pro-uPA and active uPA by SPR

The equilibrium dissociation constants (K_D) were determined by global fitting of the SPR data to a 1:1 binding model. The dissociation constants (K_D) are reported as the averages ± S.D. of 3–12 independent experimental determinations.

	Pro-uPA			Active uPA		
Antibody	**k_{on} (10^4 $M^{-1}s^{-1}$)**	**k_{off} (10^{-4} s^{-1})**	**K_D (nM)**	**k_{on} (10^4 $M^{-1}s^{-1}$)**	**k_{off} (10^{-4} s^{-1})**	**K_D (nM)**
mAb-PUK	11 ± 5*	4.3 ± 1.8*	4.3 ± 1.5*	n.b.[1]	n.b.[1]	n.b.[1]
mAb-12E6B10	n.b.[1]	n.b.[1]	n.b.[1]	32 ± 4**	15 ± 0.3**	4.5 ± 0.4**
mAb-112	12 ± 4*	0.4 ± 0.2*	0.39 ± 0.16*	0.1 ± 0.1	2.0 ± 1.2	141 ± 47
mAb-101	41 ± 22	17 ± 8	4.6 ± 1.9	24 ± 18	21 ± 15	8.4 ± 5.8

[1] No measurable binding at 200 nM protease.

* Significantly different from corresponding value for uPA ($p < 0.01$).

** Significantly different from corresponding value for pro-uPA ($p < 0.01$).

MAb-112 data were reported in [15] and shown here for comparison.

Table 2

Kinetic analysis of the binding of antibodies to pro-uPA or active uPA variants by SPR

The equilibrium dissociation constants (K_D) were determined by global fitting of the SPR data to a 1:1 binding model. The dissociation constants (K_D) are reported as the averages ± S.D. of 2–12 independent experimental determinations.

The following pro-uPA mutants showed unaltered binding to mAb-PUK: R13A, Y34A, H37A, S37dA, T39A, Y40A, V41A, S48A, R72A, L73A, N74A, F141A, G142A, K143A, N145A, S146A, T147A, D148A, L150A, P152A, Q154A, K156A, D189A, S190A, Q192A, D194A. The following uPA mutants showed unaltered binding to mAb-12E6B10: T5A, I17A, E20A, P152A, R217A, K223A, K225A. The following uPA mutants showed unaltered binding to mAb-101: K62A, E62aA, F83A, E84A, K110aA, E110bA.

Antibody	uPA variant	k_{on} $M^{-1}s^{-1} \cdot 10^4$	k_{off} $s^{-1} \cdot 10^{-4}$	K_D nM	$K_{D\text{-variant}}/K_{D\text{-wt}}$
mAb-PUK	wt pro-uPA	11 ± 5	4.3 ± 1.8*	4.3 ± 1.5	1
	pro-uPA K15A	n.b.1	n.b.1	n.b.1	-
	pro-uPA I16A	62 ± 15	148 ± 7	25 ± 7	5.8
	pro-uPA I17A	n.b.1	n.b.1	n.b.1	-
	pro-uPA E144A	n.b.1	n.b.1	n.b.1	-
	pro-uPA Y149A	n.b. 1	n.b.1	n.b.1	-
	pro-uPA Y151A	40 ± 28	133 ± 39	41 ± 17	9.6
mAb-12E6B10	wt uPA	32 ± 4	15 ± 0.3	4.5 ± 0.4	1
	uPA F21A	0.5 ± 0.4	240 ± 30	6902 ± 5486	1530
	uPA T23A	n.b.1	n.b.1	n.b.1	-
	uPA N26A	n.b.1	n.b.1	n.b.1	-
	uPA E144A	n.b.1	n.b.1	n.b.1	-
	uPA N145A	n.b.1	n.b.1	n.b.1	-
	uPA T147A	0.5 ± 0.2	7.5 ± 0.3	166 ± 56	37
	uPA D148A	n.b.1	n.b.1	n.b.1	-
	uPA Y149A	n.b.1	n.b.1	n.b.1	-
	uPA Y151A	n.b.1	n.b.1	n.b.1	-
	uPA K156A	n.b.1	n.b.1	n.b.1	-

Antibody	uPA variant	k_{on} $M^{-1}s^{-1} \cdot 10^4$	k_{off} $s^{-1} \cdot 10^{-4}$	K_D nM	$K_{D\text{-variant}}/K_{D\text{-wt}}$
	D194A	n.b.[1]	n.b.[1]	n.b.[1]	-
mAb-101	wt pro-uPA	41 ± 22	17 ± 8	4.6 ± 1.9	1
	pro-uPA E86A	n.b.[1]	n.b.[1]	n.b.[1]	-
	pro-uPA R109A	n.b.[1]	n.b.[1]	n.b.[1]	-
	pro-uPA E110dA	n.b.[1]	n.b.[1]	n.b.[1]	-

[1] No measurable binding at 200 nM protease.

mAb-112 data were reported in [15].